Postprint of: Hafeez M. B., Krawczuk M., Kottakkaran S. N., Jamshed W., Pasha A. A., A finite element analysis of thermal energy inclination based on ternary hybrid nanoparticles influenced by induced magnetic field, INTERNATIONAL COMMUNICATIONS IN HEAT AND MASS TRANSFER Vol. 135, (2022), 106074, DOI: 10.1016/j.icheatmasstransfer.2022.106074

International Communications in Heat and Mass Transfer

Maximum Transportation Growth in Energy and Solute Particles in Prandtl Martial across a Vertical 3D-Heated Surface: Simulations Achieved using by Finite Element Approach

--Manuscript Draft--

Manuscript Number:	ICHMT-D-22-00692
Full Title:	Maximum Transportation Growth in Energy and Solute Particles in Prandtl Martial across a Vertical 3D-Heated Surface: Simulations Achieved using by Finite Element Approach
Article Type:	Research Paper
Keywords:	argumentation into heat energy; thermal properties; hybrid nanoparticles; variable magnetic field; Variable thermal conductivity; variable mass diffusion
Corresponding Author:	Muhammad Bilal Hafeez Gdansk, Pomeranian POLAND
Corresponding Author Secondary Information:	
Corresponding Author's Institution:	
Corresponding Author's Secondary Institution:	
First Author:	Muhammad Bilal Hafeez
First Author Secondary Information:	
Order of Authors:	Muhammad Bilal Hafeez
	Marek Krawczuk
	Hasan Shahzad
Order of Authors Secondary Information:	
Abstract:	Current analysis simulates heat energy and concentration production into Prandtl liquid over the vertical 3D-heated plate. The involvement of Soret and Dufour's theory into concentration and energy equations are addressed. The role of hybrid nanoparticles is inserted to visualize efficiencies of particles into solute and thermal energy. The motivation of developed analysis is to optimize solute and thermal energy applications in biomedical and industrial fields. Variable thermal conductivity and variable mass diffusion are accumulated. System of developed (partial differential equations) PDEs contains concentration, momentum, and thermal energy equations within various thermal aspects. For solution, the system of (ordinary differential equations) ODEs are formulated via transformations. A finite element algorithm is adopted to analyze various aspects versus different parameters. It is observed that motion into nanoparticles particles is smaller than motion into hybrid nanoparticles. Moreover, variations of heat energy and solute particles are noticed against variation in Soret, Eckert, magnetic and Dufour number. Magnetic field parameter reduces the motion of particles. Maximum amount of thermal energy is achieved versus argument values of Eckert number, bouncy parameter and magnetic parameter. Role of variable thermal conductivity number rises growth of heat energy and 300 elements are needed for mesh-free analysis.
Suggested Reviewers:	Sami Ullah Khan COMSATS University Islamabad - Wah Campus sk_iiu@yahoo.com Expert in boundary layer and fluid flow problem
	Muhammad Irfan Quaid-i-Azam University Islamabad: Quaid-i-Azam University mirfan@math.qau.edu.pk

	expert in fem
	Umer Farooq COMSATS University Islamabad umer_farooq@comsats.edu.pk mathematical modeling in fluid flow
Opposed Reviewers:	
Additional Information:	
Question	**Response**
Please enter the **Word Count** of your manuscript	4223
In support of Open Science, International Communications in Heat and Mass Transfer offers its authors a free preprint posting service. Preprints provide early registration and dissemination of research, which facilitates early citations and collaboration. Please indicate below whether you would like to release your manuscript publicly as a preprint on the preprint server www.SSRN.com once it enters peer-review with the journal. Your choice will have no effect on the editorial process or outcome with the journal. Your preprint will remain globally available free to read whether the journal accepts or rejects your manuscript. For more information about posting to www.SSRN.com, please consult the SSRN Terms of Use and FAQs.	NO, I don?t want to share my research early and openly as a preprint.

Maximum Transportation Growth in Energy and Solute Particles in Prandtl Martial across a Vertical 3D-Heated Surface: Simulations Achieved using by Finite Element Approach

Muhammad Bilal Hafeez[a], Marek Krawczuk[a], Hasan Shahzad[b]

[a]Gdansk University of Technology, Faculty of Mechanical Engineering and Ship Technology, Institute of Mechanics and Machine Design, Narutowicza 11/12, 80-233 Gdańsk, Poland

[b]Faculty of Materials and Manufacturing, College of Mechanical Engineering and Applied Electronics Technology, Beijing University of Technology, China.

Abstract: Current analysis simulates heat energy and concentration production into Prandtl liquid over the vertical 3D-heated plate. The involvement of Soret and Dufour's theory into concentration and energy equations are addressed. The role of hybrid nanoparticles is inserted to visualize efficiencies of particles into solute and thermal energy. A phenomenon of viscous dissipation and variable magnetic field is taken out. The motivation of developed analysis is to optimize solute and thermal energy applications in biomedical and industrial fields. Variable thermal conductivity and variable mass diffusion are accumulated. System of developed (partial differential equations) PDEs contains concentration, momentum, and thermal energy equations within various thermal aspects. For solution, the system of (ordinary differential equations) ODEs are formulated via transformations. A finite element algorithm is adopted to analyze various aspects versus different parameters. It is observed that motion into nanoparticles particles is smaller than motion into hybrid nanoparticles. Moreover, variations of heat energy and solute particles are noticed against variation in Soret, Eckert, magnetic and Dufour number. The general conclusion is that production of heat energy is significantly higher compared to the case for hybrid nanostructures. Magnetic field parameter reduces the motion of particles. Maximum amount of thermal energy is achieved versus argument values of Eckert number, bouncy parameter and magnetic parameter. Role of variable thermal conductivity number rises growth of heat energy and 300 elements are needed for mesh-free analysis.

Keywords: porous surface; argumentation into heat energy; thermal properties; hybrid nanoparticles; variable magnetic field; variable thermal conductivity; variable mass diffusion; Prandtl matrial.

1. Introduction

Due to advancements in technology, the synthesis of solid particles of nano-size has become possible. These nanoparticles have been used in many advanced engineering applications. In this sense, transportations of heat, cooling, and thermal systems, engine oil usage, electronic devices, medical sciences, etc. are the sectors where nanofluids (fluid with nanoparticles) play a significant role. The practical direct applications of nanofluids have motivated engineers and scientists to investigate the dynamics of fluids with nanoparticles. Here, let us describe some recent and relevant investigations. For instance, Dogonchi et al. [1] discussed the simultaneous impact of thermal radiations, thermal relaxation, and dispersion of nanoparticles on heat transfer in fluid over a stretchable surface. Sadeghi et al. [2] analyzed the role of heat transfer in water enclosures with wavy walls. They also analyzed the impact of internal heat generation on heat transfer enhancement in natural convective flow. Nazir et al. [3] modeled flow and thermal analysis in hyperbolic tangent liquid inserting hybrid nanostructures past heated plate. They adopted finite element approach to address various aspects. Zahra et al. [4] investigated the effects of thermal radiations heat transfer with a solar system subjected to the flow with nanoparticles. Sheikholeslami and Ganji [5] discussed heat transfer in ferrofluid with nanoparticles exposed to the magnetic field. Zeeshan and Bhargav [6] investigated the influence of dispersion of and in fluid on heat transfer in the fluid using the molecular dynamics approach. Sajjad et al. [7] analyzed the influence of the Darcy-Forchheimer porous medium and nanoparticles on heat transfer in fluid over a moving surface.

It may be therefore stated that it becomes the universal truth that the effectiveness of thermal conductivity of fluid due to dispersion of a single kind of nanoparticles is lesser than the effectiveness of thermal conductivity of fluid due to the dispersion of hybrid nanoparticles. Therefore, the usage of hybrid nanostructures for optimized thermal enhancement of the working fluid is recommended. Due to this significant reason, several studies on this topic have been conducted. For example, Nazir et al. [8] studied comparison among hybrid nanoparticles and nanomaterials in base fluid (ethylene glycol) considering Carreau Yasuda martial and thermal

properties. Nazir et al. [9] discussed the role of Williamson liquid in thermal energy and concentration involving hybrid nanoparticles towards melting surface via non-Fourier's theory. Dogonchi et al. [10] analyzed the role of hybrid nanoparticles on the thermal efficiency of fluid between two parallel plates subjected to thermal radiations. Chamkha et al. [11] published on the simultaneous influence of hybrid nanoparticles, magnetic field, and rotations of walls on the transfer of heat. Masayebidarched et al. [12] performed theoretical analysis for the thermal enhancement in fluid with hybrid nanoparticles. Similar works published on the role of hybrid nanoparticles on thermal enhancement can be seen in references [13-15]. Many Researchers like [16-22] did examinations on heat enhancement of nanofluids by blending more than one kind of nanoparticles into base liquid. These examined are engaged to the effects of actual factors, for example, joule heating effect, buoyancy force, and magnetic effect on the heat enhanced of nanofluids. Researchers are recommended to concentrate on these most recent specialists as they likewise caught diverse mathematical impacts, the porosity of the medium, and extending contracting of plates in no-slip effect. Effects of Dufour and Soret were studied in [23] by the influence of mechanism of solute and thermal Characteristics in a Casson Hybrid nanofluid. We Observed the Heat transfer improvement through nanofluids with applications in a vehicle radiator. and analysis of significant production of thermal energy in partially Ionized Hyperbolic Tangent Material Based on Ternary Hybrid in [24].

To conclude, the latest development on the simultaneous transfer of heat and mass has revealed that compositional gradients are a favorable factor for the transfer heat. Similarly, the temperature gradient is supporting to enhance mass transfer in fluids. The transfer of heat due to compositional differences of solute is termed the Dufour effect whereas the transfer of mass due to temperature gradient is called the Soret effect. These effects have been studied theoretically in recent years. For instance, Hayat and Nawaz [16] studied the combined effects of temperature and concentration gradients on mixed convection heat and mass transport in partial ion, second-grade fluid subjected magnetic field. Nawaz et al. [17] studied Soret and Dufour's effects on heat and mass transfer in an axisymmetric flow between two moving surfaces. Subrat et al. [18] examined Soret and Dufour's effects on transport phenomenon in thermochemical flow. Iskandar et al. [19] analyzed the combined effects of Soret and Dufour due to the suspension of nano-

sized particles on heat and mass transfer inflow over a moving thin needle. Ambreen et al. [20] also examined the impact of temperature and concentration gradients.

A significant literature review demonstrates that three dimensional developing modemodels view of heat energy and mass diffusion in the presence of hybrid-Prandtl nanofluid over a vertical stretching heated surface is not investigated yet. The mathematical model is developed as more complex due to the involvement of Soret and Dufour effects. A variable magnetic field is inserted with heat source and Joule heating phenomena. Furthermore, Variable properties in view of thermal conductivity and mass diffusion along hybrid nanofluid are accumulated. Developing complex model is simulated by finite element. Therefore, this new investigation consists of five Sections showing some possible solutions. The problem formulation is given in Section 2. The numerical method is briefly explained in Section 3. The outcomes are discussed in Section 4. Section 5 concludes this study.

2. Flow analysis

Features of thermal energy and solute particles into Prandtl liquid inserting hybrid nanostructures towards a heated vertical surface area considered under the impact of variable magnetic field. A porous surface is taken to know characterizations of motion and thermal energy of particles along with Dufour and Soret influences in the presence of temperature dependent mass diffusion and thermal conductivity are addressed. Composite of Ag and Cu is called hybrid nanostructure, while Ag a is known as nanoparticle. Thermal properties of Ag and Cu is illustrated in Table 1. The schematic behavior of the current model is presented in Fig. 1. It noticed that x-axis is taken along vertical direction and y-axis is assumed along horizontal direction while magnetic field is inserted along y-direction.

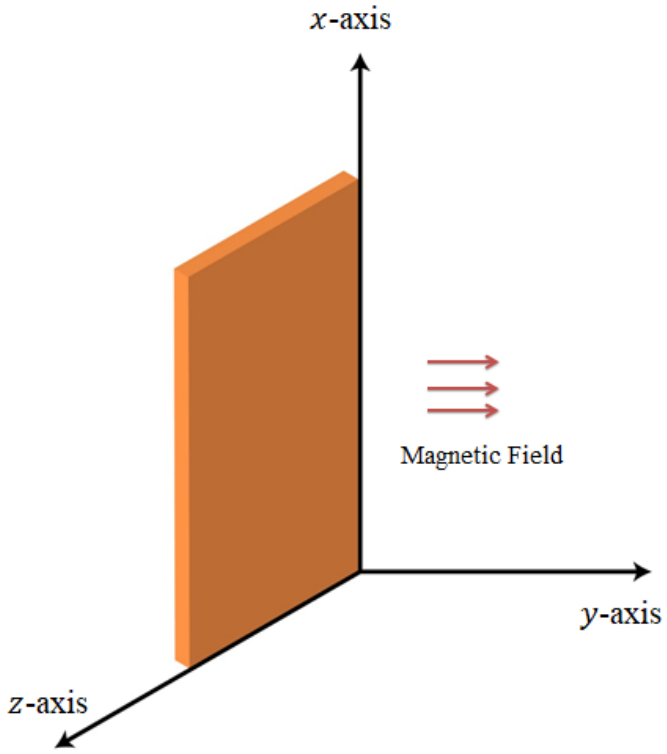

Figure 1. 3D vertical surface.

PDEs, describing the problem, can be stated as

$$\frac{\partial u}{\partial x}+\frac{\partial v}{\partial y}+\frac{\partial w}{\partial z}=0, \tag{1}$$

$$u\frac{\partial u}{\partial x}+v\frac{\partial u}{\partial y}+w\frac{\partial u}{\partial z}=\left(\beta_{hnf}\right)_T g^*(T-T_\infty)+\left(\beta_{hnf}\right)_C g^*(C-C_\infty)-$$

$$-\frac{\sigma_{hnf}}{\rho_{hnf}}B_o^2A^2(x+y)^{-\frac{2}{3}}u-\mu_{hnf}\frac{u}{K_1}+\nu_{hnf}\left[\frac{A}{C}\frac{\partial^2 u}{\partial z^2}+\frac{A}{2C^3}\frac{\partial^2 u}{\partial z^2}\left(\frac{\partial u}{\partial z}\right)^2\right], \tag{2}$$

$$u\frac{\partial v}{\partial x}+v\frac{\partial v}{\partial y}+w\frac{\partial v}{\partial z}=\nu_{hnf}\frac{\partial^2 v}{\partial z^2}+\left(\beta_{hnf}\right)_T g^*(T-T_\infty)+\left(\beta_{hnf}\right)_C g^*(C-C_\infty)-$$

$$-\frac{\sigma_{hnf}}{\rho_{hnf}}B_o^2A^2(x+y)^{-\frac{2}{3}}v-\mu_{hnf}\frac{v}{K_1}+\nu_{hnf}\left[\frac{A}{C}\frac{\partial^2 v}{\partial z^2}+\frac{A}{2C^3}\frac{\partial^2 v}{\partial z^2}\left(\frac{\partial v}{\partial z}\right)^2\right], \tag{3}$$

$$u\frac{\partial T}{\partial x}+v\frac{\partial T}{\partial y}+w\frac{\partial T}{\partial z}=\frac{1}{\left(\rho c_p\right)_{Thnf}}\frac{\partial}{\partial z}\left(K_{Thnf}(T)\frac{\partial T}{\partial z}\right)+\frac{Q_0}{\left(\rho c_p\right)_{hnf}}(T-T_\infty)+\frac{DK_T}{C_sC_p}\frac{\partial^2 C}{\partial z^2}$$

$$+\frac{\sigma_{hnf}B_o^2A^2(x+y)^{-\frac{2}{3}}}{\left(\rho c_p\right)_{hnf}}(u^2+v^2)$$

$$u\frac{\partial C}{\partial x}+v\frac{\partial C}{\partial y}+w\frac{\partial C}{\partial z}=\frac{\partial}{\partial z}\left(D_{hnf}\frac{\partial T}{\partial z}\right)+\frac{D_T}{T_\infty}\frac{\partial^2 T}{\partial z^2}, \tag{5}$$

For system Eqs. 1-5 the BCs are

$$\left.\begin{array}{c} u=U_w\left(=a(x+y)^{\frac{1}{3}}\right), v=V_w\left(=b(x+y)^{\frac{1}{3}}\right), w=0 \\ T=T_w\left(=cT_o(x+y)^{\frac{2}{3}}+T_\infty\right), C=C_w\left(=dC_o(x+y)^{\frac{2}{3}}+C_\infty\right) \quad as\ y=0 \\ u=0, v=0, T\rightarrow T_\infty, C\rightarrow C_\infty \qquad\qquad as\ y\rightarrow\infty \end{array}\right\} \tag{6}$$

Correlations among hybrid nanostructures and nanomaterial in ethylene glycol are

$$\left.\begin{array}{c} \rho_{hnf}=\left[(1-\phi_2)\left\{(1-\phi_1)\rho_f+\phi_1\rho_{s_1}\right\}\right]+\phi_2\rho_{s_2}, \rho_{nf}=(1-\phi)\rho_f+\phi\rho_s \\ \left(\rho C_p\right)_{nf}=(1-\phi)\left(\rho C_p\right)_f+\phi\left(\rho C_p\right)_s, \\ \left(\rho C_p\right)_{hnf}=\left[(1-\phi_2)\left\{(1-\phi_1)\left(\rho C_p\right)_f+\phi_1\left(\rho C_p\right)_{s_1}\right\}\right]+\phi_1\left(\rho C_p\right)_{s_2} \end{array}\right\}$$

$$\left.\begin{array}{c} \frac{k_{nf}}{k_f}=\left\{\frac{k_s+(n+1)k_f-(n-1)\phi\left(k_f-k_s\right)}{k_s+(n-1)k_f+\phi\left(k_f-k_s\right)}\right\}, \mu_{nf}=\frac{\mu_f}{(1-\phi)^{2.5}} \\ \mu_{nf}=\frac{\mu_f}{(1-\phi_2)^{2.5}(1-\phi_1)^{2.5}}, \frac{\sigma_{hnf}}{\sigma_f}=\left(1+\frac{3(\sigma-1)\phi}{(\sigma+2)-(\sigma-1)\phi}\right) \end{array}\right\} \tag{7}$$

$$\left.\begin{array}{c} \frac{k_{hnf}}{k_{bf}}=\left\{\frac{k_{s_2}+(n-1)k_{bf}-(n-1)\phi_2\left(k_{bf}-k_{s_2}\right)}{k_{s_2}+(n-1)k_{bf}-\phi_2\left(k_{bf}-k_{s_2}\right)}\right\} \\ \frac{\sigma_{hnf}}{\sigma_f}=\left(\frac{\sigma_{s_2}+2\sigma_f-2\phi_2\left(\sigma_{bf}-\sigma_{s_2}\right)}{\sigma_{s_2}+2\sigma_f+\phi_2\left(\sigma_{bf}-\sigma_{s_2}\right)}\right) \end{array}\right\}$$

Thermal conductivity and mass diffusion based on temperature are defined as

$$K_{hnf}(T)=K_{hnf}\left(1+\epsilon_1\frac{T-T_\infty}{T_w-T_\infty}\right), \tag{8}$$

$$D_{hnf}(T)=K_{hnf}\left(1+\epsilon_2\frac{T-T_\infty}{T_w-T_\infty}\right),$$

Next, the similarity transformation are

$$\left.\begin{aligned} u = a(x+y)^{\frac{1}{3}}, v = a(x+y)^{\frac{1}{3}}, \eta = \sqrt{\frac{a}{\nu_f}}(x+y)^{-\frac{1}{3}}z, \\ w = -\sqrt{a\nu_f}\,(x+y)^{-\frac{1}{3}}\left(\frac{2}{3}(f+g) - \frac{1}{3}\eta(f'+g')\right), \theta = \frac{T-T_\infty}{T_w-T_\infty}, \phi = \frac{C-C_\infty}{C_w-C_\infty} \end{aligned}\right\} \tag{9}$$

Using similarity transformation in Eqs. $(1)-(6)$, we have

$$\left.\begin{aligned} \frac{\nu_{hnf}}{\nu_f}(\alpha_1 f''' + \alpha_2 f''^2 f''') - \frac{1}{3}(f'+g')f' + \frac{2}{3}(f+g)f'' + (Gr)_t\theta \\ +(Gr)_c\phi - \left(\frac{\sigma_{hnf}}{\sigma_f}\right)\left(\frac{\rho_f}{\rho_{hnf}}\right)Mf' - \left(\frac{\mu_{hnf}}{\mu_f}\right)K^*f' = 0 \\ f'(0) = 1,\ \ f(0) = 0,\ \ f'(\infty) \to 0, \end{aligned}\right\}$$

$$\left.\begin{aligned} \frac{\nu_{hnf}}{\nu_f}(\alpha_1 g''' + \alpha_2 g''^2 g'') - \frac{1}{3}(f'+g')g' + \frac{2}{3}(f+g)g'' + (Gr)_t\theta \\ +(Gr)_c\phi - \left(\frac{\sigma_{hnf}}{\sigma_f}\right)\left(\frac{\rho_f}{\rho_{hnf}}\right)Mg' - \left(\frac{\mu_{hnf}}{\mu_f}\right)K^*g' = 0 \\ g'(0) = \beta,\ \ g(0) = 0,\ \ g'(\infty) \to 0, \end{aligned}\right\} \tag{10}$$

$$\left.\begin{aligned} \frac{K_{hnf}}{K_f}[(1+\epsilon_1\theta)\theta'' + \epsilon_1(\theta')^2] + \left(\frac{(\rho c_p)_{hnf}}{(\rho c_p)_f}\right)\frac{2}{3}Pr(f+g)\theta' - \left(\frac{(\rho c_p)_{hnf}}{(\rho c_p)_f}\right)\frac{2}{3}Pr(f'+g')\theta \\ -Pr\beta^*\theta + \left(\frac{(\rho c_p)_{hnf}}{(\rho c_p)_f}\right)DuPr\phi'' + \left(\frac{\sigma_{hnf}}{\sigma_f}\right)MPrEc(f'+g')^2 = 0 \\ \theta(0) = 1, \qquad \theta(\infty) \to 0 \end{aligned}\right\},$$

$$\left.\begin{aligned} \frac{D_{hnf}}{D_f}[(1+\epsilon_1\varphi)\varphi'' + \epsilon_2\varphi'\theta'] + \frac{2}{3}Sc(f+g)\phi' - \frac{2}{3}Sc(f'+g')\phi + SrSc\theta'' = 0 \\ \phi(0) = 1, \phi(\infty) \to 0 \end{aligned}\right\}, \tag{11}$$

The dimensionless numbers and defined here

$$\left.\begin{aligned} (Gr)_t = \frac{(\beta_{hnf})_T g^* c T_0}{a^2}\ , (Gr)_c = \frac{(\beta_{hnf})_C g^* d C_0}{a^2},\ \ M = \frac{\sigma_f}{\rho_f}\frac{{B_0}^2 A^2}{a},\ K^* = \frac{\mu_f}{a k_1}, \\ Ec = \frac{1}{(c_p)_f}\frac{a^2}{c T_0}\ ,\ \beta^* = \frac{Q_0}{a(\rho c_p)_f}\ , Du = \frac{D K_T d C_0}{C_s C_p V_f c T_0}, Sc = \frac{V_f}{d_f}\ \ , Sr = \frac{D_T T_0}{(T_\infty C_0) V_f}, \end{aligned}\right\}, \tag{12}$$

For practical purposed model parameters used in this study are summarized in Table 1.

Table 1. Thermal properties of ethylene glycol, silver and MoS_2.

MoS_2	Ag	$C_2H_6O_2$
$\rho = 5060$	$\rho = 10490$	$\rho = 1113.5$
$C_p = 397.21$	$C_p = 235$	$C_p = 2430$
$k = 904.4$	$k = 429$	$k = 0.253$
$\beta = 2.8424 \times 10^{-5}$	$\beta = 1.89 \times 10^{-5}$	$\beta = 5.8 \times 10^{-4}$
$\sigma = 2.09 \times 10^{-5}$	$\sigma = 6.30 \times 10^{7}$	$\sigma = 4.3 \times 10^{-5}$

The surface forces are captured as

$$C_{fx} = \frac{\frac{\partial u}{\partial z}\Big|_{z=0}}{\rho_f (U_w)^2} = \frac{(1-\phi_1)^{-2.5}}{(1-\phi_2)^{2.5}(Re)^{1.5}} [\alpha_1 f''(0) + \alpha_2 (f'''(0))^3], \tag{13}$$

$$C_{gy} = \frac{\frac{\partial v}{\partial z}\Big|_{z=0}}{\rho_f (U_w)^2} = \frac{(1-\phi_1)^{-2.5}}{(1-\phi_2)^{-2.5}(Re)^{1.5}} [\alpha_1 g''(0) + \alpha_2 (g'''(0))^3]. \tag{14}$$

Nusselt number is

$$Nu = -\frac{(x+y) K_{hnf} \frac{\partial T}{\partial y}\Big|_{y=0}}{k_f (T - T_\infty)} = -\frac{K_{hnf}}{k_f (Re)^{1.5}} \theta'(0), \tag{15}$$

the rate of mass diffusion is

$$Sh = \frac{(x+y) D_{hnf} \frac{\partial C}{\partial y}\Big|_{y=0}}{D_f (C - C_\infty)} = -\frac{D_{hnf}}{D_f (Re)^{1.5}} \phi'(0), \tag{16}$$

where $Re = \frac{x U_w}{\nu_f}$, the Reynolds number.

3. Numerical method

FEM (finite element method) is used to obtain solution of the presented problem. The working rules of FEM are given below [27-31]. Some limitations on finite element method are listed below.

Finite element method is observed as more complex in view of understanding rather than others numerical methods;

Finite element method can be expensive in term of computational cost as compared to other methods;

Large data is needed for mesh free analysis.

The residual equations are constructed.

The residual is integrated over the typical element of the discretized domain.

The weighted residual integrals are approximated using Galerkin approach and stiffness matrices are derived.

The rules of assembly of elements are followed and nonlinear system of equation is linearized. The linearized system is solved under computational tolerances 10^{-3}.

The convergence is checked, and grid independent results are obtained. The criterion of error analysis is used.

$$\left|\frac{L^{i+1}-L^{i}}{L^{i}}\right|<10^{-5}. \tag{17}$$

In examples the parametric study is elaborated to study heat energy and mass transfer in 3D flow of Newtonian fluid showing the influences of heat generation, porous medium, viscous dissipation, temperature gradient, rate of mass diffusion and Joule heating. Table 2 reveals mesh free analysis of problem testing by 300 elements.

Table. 2 Grid independent study of concentration, velocities and temperature observing by 300 elements.

Number of elements	$f'\left(\frac{\eta_{max}}{2}\right)$	$g'\left(\frac{\eta_{max}}{2}\right)$	$\theta\left(\frac{\eta_{max}}{2}\right)$	$\phi\left(\frac{\eta_{max}}{2}\right)$
30	0.7840956617	0.003662478537	0.0036624785	0.0001068718
60	0.8208393123	0.0900095316 4	0.1110267939	0.0050688393 4
90	0.8299235799	0.0026505129 86	0.0134215580 3	0.0000569166 0
120	0.69097296	0.0004285360	0.010391537	0.045448244

	70	556	13	77
150	0.6949838844	0.0004160495348	0.0103312436	0.0450001868
180	0.6979030185	0.0004100790678	0.0102944276	0.0447782715
210	0.7002801242	0.0004086029651	0.0102719213	0.0447074739
240	0.7023798401	0.0004105345687	0.0102590255	0.0447478444
270	0.7043301851	0.0004151139823	0.0102529056	0.0448720567
300	0.7061806472	0.0004216405675	0.0102515276	0.0450558593

3. Results and discussion

The parametric study is offered to explore the physics of the problem explained in the previous section. Numerical solution is obtained by using fractional finite element method**.** The aspects of heat energy and mass diffusion in non-Newtonian flow over a surface with temperature (variable) and wall concentration (variable) is modeled and mathematical model is solved numerically using FEM. As yield stress is the characteristics due to which fluid resists against deformation until certain amount of applied stress reaches. As yield stress increases, the fluid ability to resist against the applied stress to attain its equilibrium state, therefore, a decrease in the velocity field (in both $\boldsymbol{x}$ and $\boldsymbol{y}$ -components) is observed (see Figs. 2 and 3). Figures 2 and 5 are prepared to capture the role of fluid parameter on velocity curves. It is noticed that fluid becomes thin versus the higher impacts of fluid parameter.

The various numerical experiments are performed with different samples of parametric values. Some crucial observations are obtained from the numerical experiments. It is important to note that dashed curves are associated with flow, heat transfer and mass diffusion in nanofluid (Cu-nanofluid) whereas solid curves are associated with flow, heat transfer and mass transport in hybrid nanofluid (Cu - Ag -nanofluid). The increase in the magnitude of resistive force is

captured first. Obviously, the flow in both x- and y- directions decelerates - see Figs. 4 and 5). Moreover, the parameter k^* associated with porous medium resistivity against the flow of fluid and its impact on motion of fluid particles is shown in Figs. 6 and 7- decreasing behavior of velocity can be seen from Figs. 6 and 7. These Figures also show that hybrid nano-Casson fluid experiences more resistance by the porous medium than the mono nano-Casson fluid. The viscous region for mono, nano-Casson fluid is wider than that for hybrid nano-Casson fluid.

Role of magnetic field versus fluid flow: The direct relation is addressed to magnetic field and Lorentz force. The influence of Lorentz force on flow can be determined by variation of M. The large values of M make an increment in the opposing effect of Lorentz force. Therefore, flow experiences the retardation due to Lorentz force. (see Figs. 6 and 7). Thus, boundary layer thickness is tackled by varying magnetic field (the intensity of applied). It is also noted that Lorentz force for the case of flow of Cu - Ag -nanofluid is greater than the Lorentz force in case of flow of Cu -nanofluid.

Temperature field versus variation of crucial model parameters: The effects of $Du, (Gr)_t, M, Pr, \beta^*$, and Ec versus thermal energy for both nanfluid (Cu -nanofluid) and hybrid nanofluid (Cu - Ag -nanofluid) are examined. The observed influence of these parameters is shown by Figs 8-12, respectively. The parameter Du is called Dufour number. It appears in the dimensionless form of energy equation when transcript of thermal energy due to concentration gradient is considered. It measures the transfer of heat energy due to compositional differences caused by nanoparticles and solute diffused in the fluid. The effects of Du on temperature of Cu -nanofluid and Cu - Ag – hybrid nanofluid are shown by Figures 8. The temperature of both types of fluids has increasing tendency as a function of Du. The influence of Du on temperature of Cu -nanofluid is smaller than that on the temperature of and Cu - Ag -nanofluid. The effects of Buoyancy force on temperature of and Cu -nanofluid and and Cu - Ag - nanfluid is represented by Fig. 9. $(Gr)_\in > 0$ is the case when the Buoyancy force is positive, and flow is assisted by this force. However, $(Gr)_t < 0$, the case when Buoyancy force is negative, the flow in this case is called opposing flow. The Joule heating phenomenon is a phenomenon in which heat is generated due to conversion and that heat adds to the medium like fluid. Consequently, temperature due to Joule heating is shown by Fig. 10. It is also noted that Joule heating phenomenon in hybrid nanofluid is stronger than that in Cu -nanofluid (mono-fluid). Moreover, the parameter β^*, which appears a result of non-dimensionlizing the heat generation term in

energy equation increase in heat generation. This generated heat adds to the fluid and consequently, its temperature rises. This observation can be confirmed from Fig. 11. The viscous dissipation causes a significant rise in temperature of fluids (-nanofluid and Cu - Ag – nanofluid). It is found from simulations that viscous dissipation in nanofluid Cu -nanofluid is grater than that in hybrid nanofluid Cu - Ag – nanofluid. These observations can be noticed from Fig. 12.

Role of mass diffusion: The parameters Sr, $(Gr)_c$, and Sc, respectively, determine the impact of temperature gradient, Buoyancy force due to concentrations difference and diffusion coefficient on concentration field. Their influence on concentrations can be seen from Figs. 13-15. Hence an increasing effect of Sr and $(Gr)_c$ can be noticed in Figs 13 and 15. On the other hand, concentration field decreases as a function Sc.

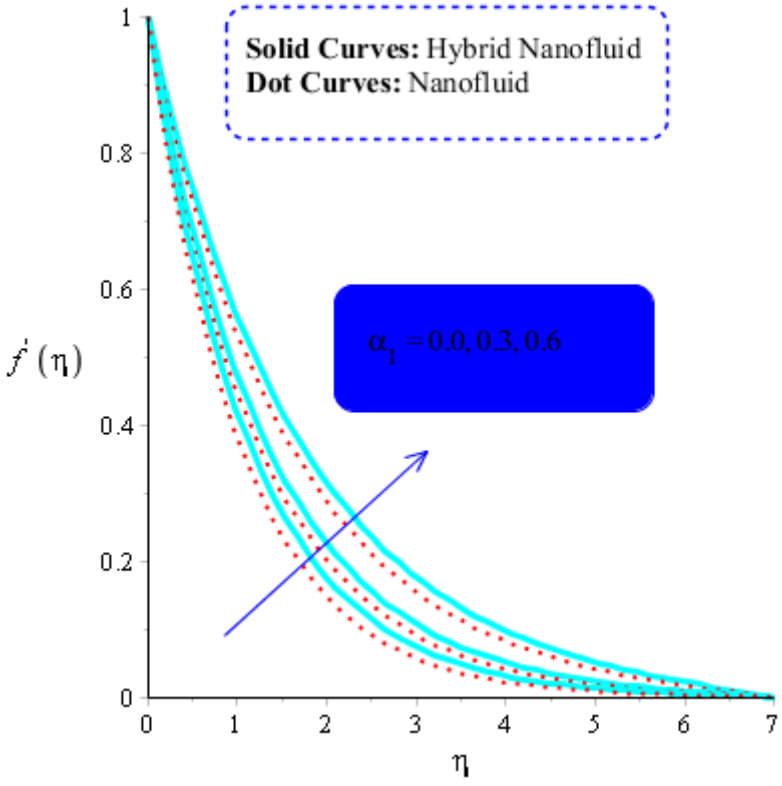

Figure 2. Influence of α_1 on f' when

$(Gr)_t = 0.7, Pr = 3, Sc = 0.6, K^* = 0.5, Ec = 0.01, (Gr)_c = 0.5, M = 0.2,\ \beta^* = 0.2, Sr = 0.7,$ and $Du = 0.2, Du = 0.2, \epsilon_1 = 0.4, \epsilon_2 = 0.5, \alpha_2 = 5.0.$

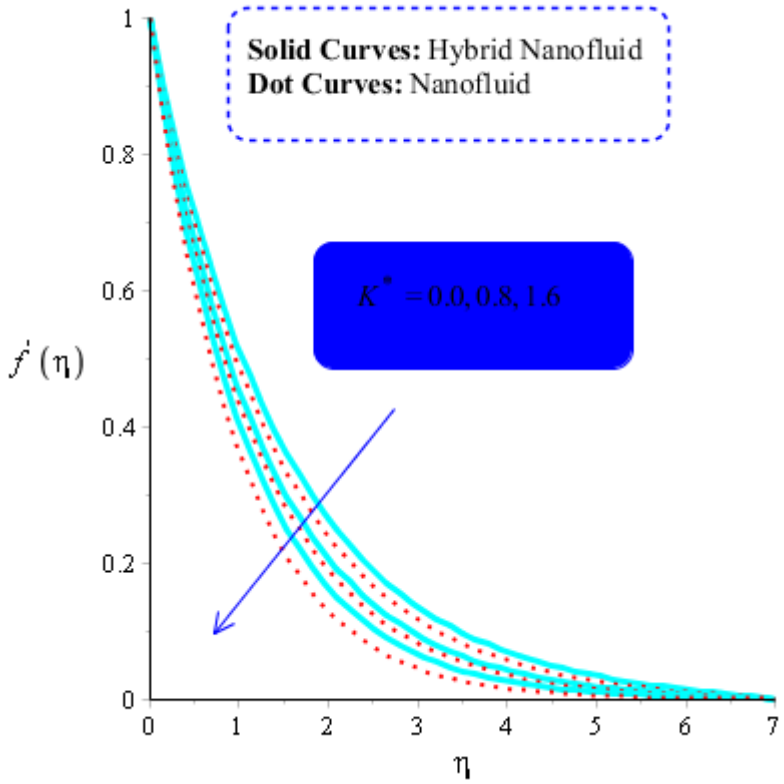

Figure 3. Influence of K^* on f' when $(Gr)_t = 0.5, Pr = 4, Sc = 5, \beta = 0.2, Ec = 0.001, (Gr)_c = 0.3, M = 0.5, \beta^* = 0.2, Sr = 0.1,$ and $Du = 0.2, \epsilon_1 = 0.7, \epsilon_2 = 0.5, \alpha_1 = 0.5, \alpha_2 = 5.0.$

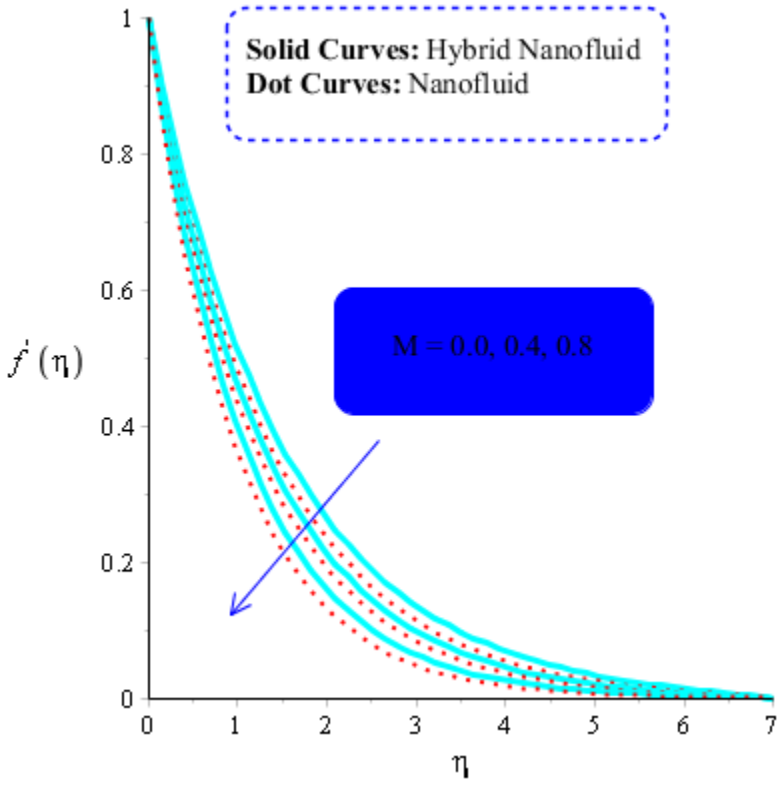

Figure 4: Influence of M on f' when $(Gr)_t = 0.7, Pr = 8, Sc = 5, \beta = 0.2, Ec = 0.1, (Gr)_c = 0.5, K^* = 0.1, \beta^* = 0.2, Sr = 0.1,$ and $Du = 0.2, \epsilon_1 = 0.3, \epsilon_2 = 0.7, \alpha_1 = 0.5, \alpha_2 = 3.0.$

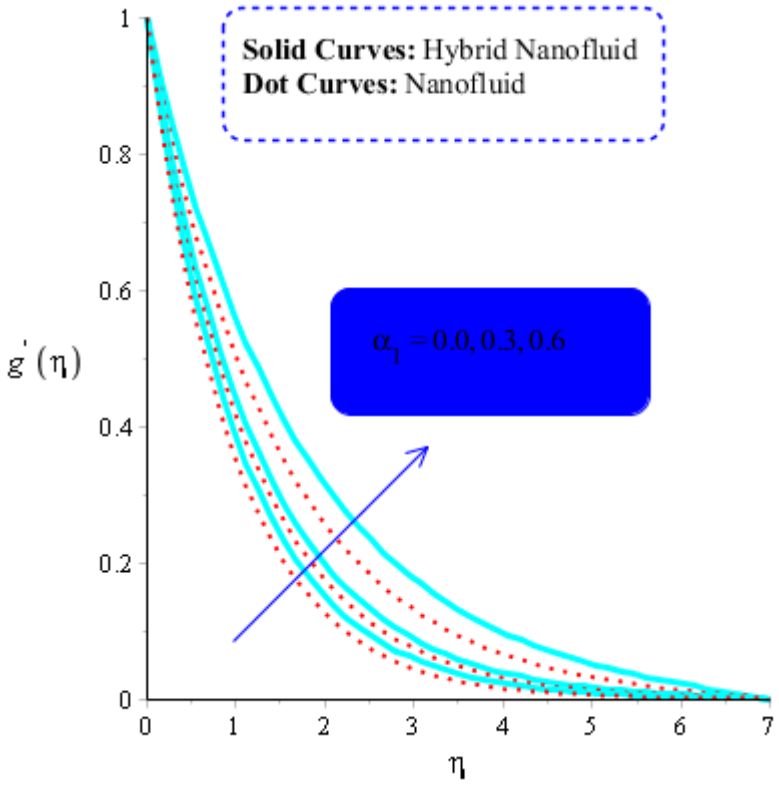

Figure 5: Influence of α_1 on g' when $(Gr)_t = 0.5, Pr = 5, Sc = 5, K^* = 0.1, Ec = 0.001, (Gr)_c = 0.7, M = 0.5, \beta^* = 0.2, Sr = 0.1,$ and $Du = 0.2, Du = 0.2, \epsilon_1 = 0.3, \epsilon_2 = 0.5, \alpha_2 = 3.0.$

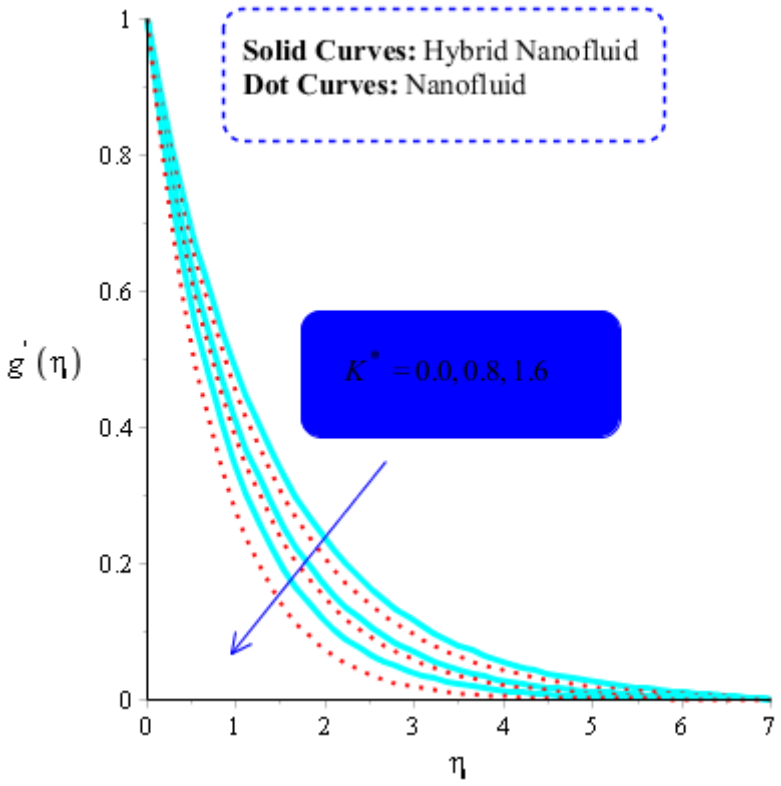

Figure 6: Influence of K^* on g' when $(Gr)_t = 0.5, Pr = 5, Sc = 5, \beta = 0.2, Ec = 3, (Gr)_c = 0.3, M = 0.5, \beta^* = 0.2, Sr = 0.1,\ Du = 0.8,\ \epsilon_1 = 0.3, \epsilon_2 = 0.3, \alpha_1 = 0.5, \alpha_2 = 3.0.$

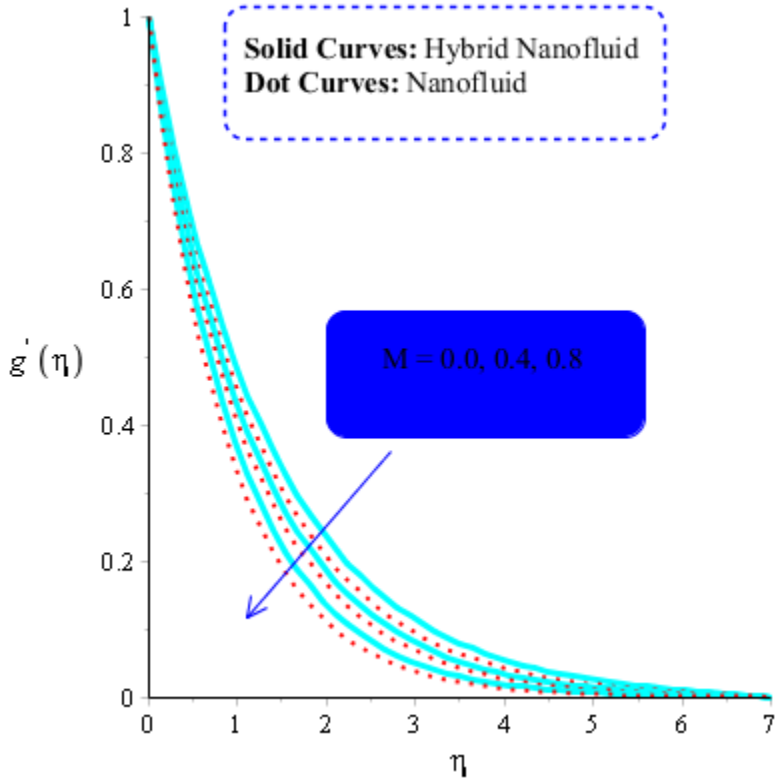

Figure 7: Influence of M on g' when $(Gr)_t = 0.5, Pr = 4, Sc = 5, \beta = 0.2, Ec = 0.001, (Gr)_c = 0.3, K^* = 0.1, \beta^* = 0.2, Sr = 0.1,$ and $Du = 0.2, Du = 0.2, \epsilon_1 = 0.3, \epsilon_2 = 0.5, \alpha_1 = 0.5, \alpha_2 = 3.0.$

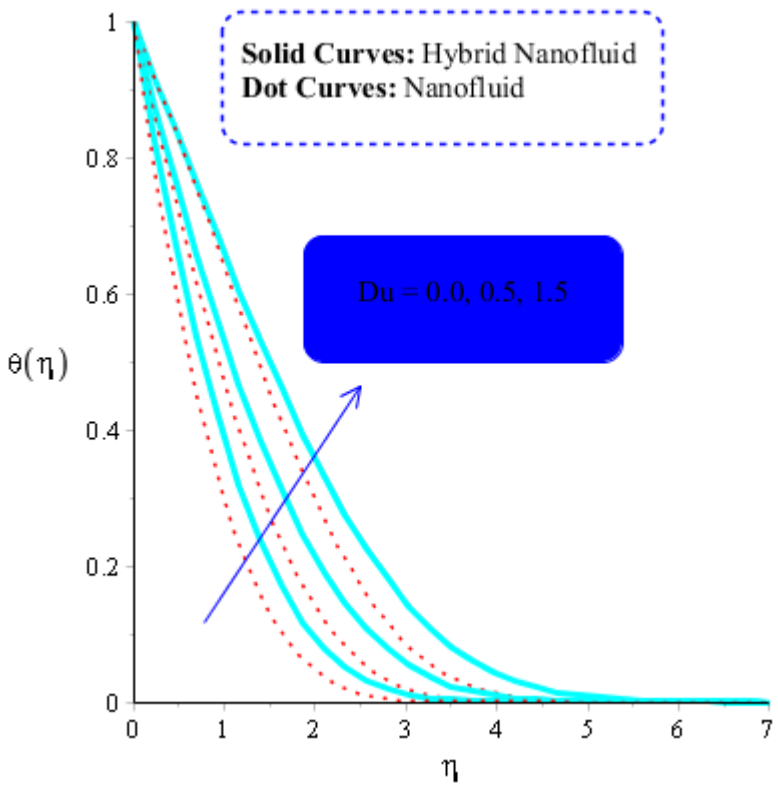

Figure 8: Influence of Du on θ when $(Gr)_t = 5, Pr = 7, Sc = 0.4, \beta = 0.2, Ec = 0.001, (Gr)_c = 0.3, K^* = 0.1, \beta^* = 0.2, Sr = 0.1, M = 0.5, Du = 0.2, \epsilon_1 = 0.3, \epsilon_2 = 0.5, \alpha_1 = 0.5, \alpha_2 = 3.0.$

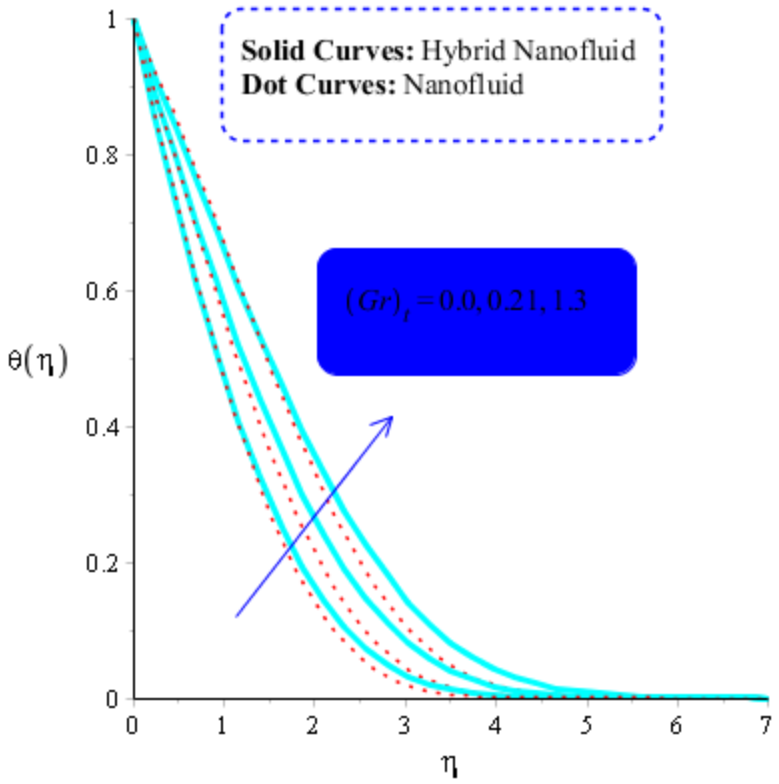

Figure 9: Influence of $(Gr)_t$ on θ when $Du = 0.3, Pr = 4, Sc = 5, \beta = 0.7, Ec = 0.01, (Gr)_c = 0.3, K^* = 0.1, \beta^* = 0.2, Sr = 0.1,\ M = 0.5, Du = 0.2, \epsilon_1 = 0.3, \epsilon_2 = 0.5, \alpha_1 = 0.7, \alpha_2 = 3.0.$

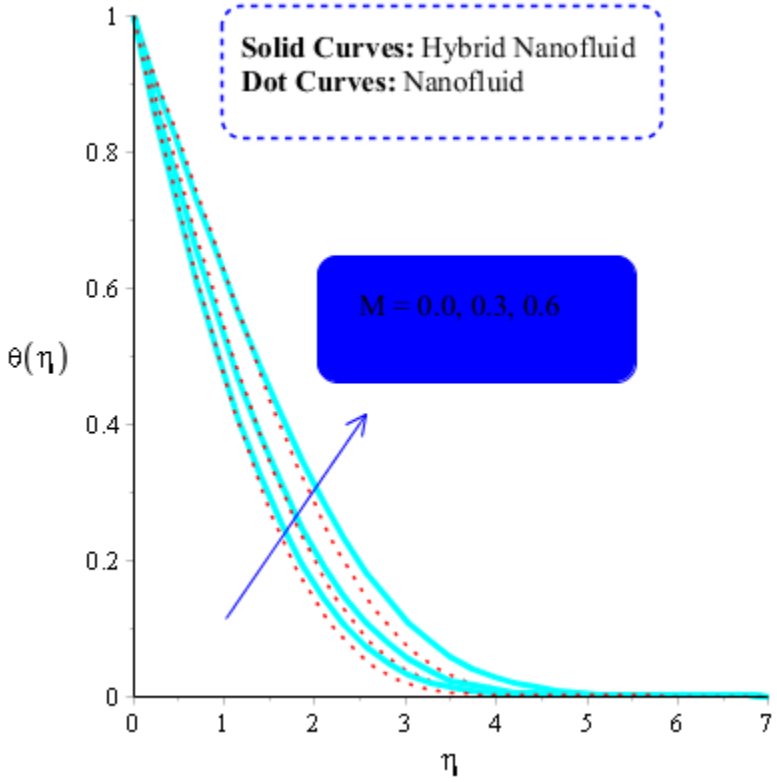

Figure 10: Influence of M on θ when $Du = 0.2, Pr = 4, Sc = 5, \beta = 0.2, Ec = 0.001, (Gr)_c = 0.3, K^* = 0.1, \beta^* = 0.2, Sr = 0.1, (Gr)_t = 0.5, Du = 0.2, \epsilon_1 = 0.3, \epsilon_2 = 0.5, \alpha_1 = 0.5, \alpha_2 = 3.0$.

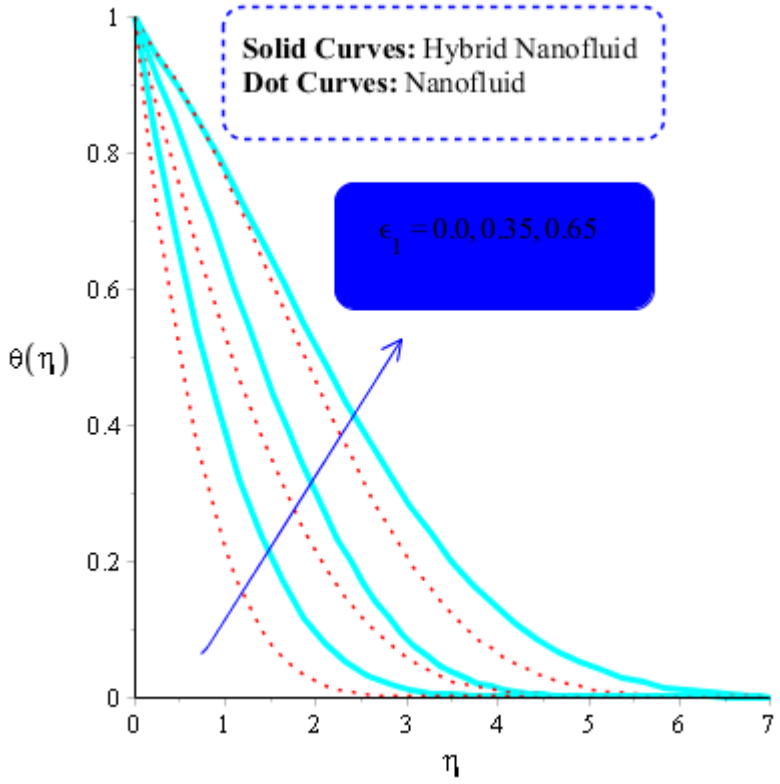

Figure 11: Influence of ϵ_1 on θ when $Du = 0.2, M = 0.5, Sc = 5, \beta = 0.2, Ec = 0.001, (Gr)_c = 0.3, K^* = 0.1, Pr = 4, Sr = 0.1, (Gr)_t = 0.5, Du = 0.2, \epsilon_2 = 0.5, \alpha_1 = 0.5, \alpha_2 = 3.0$.

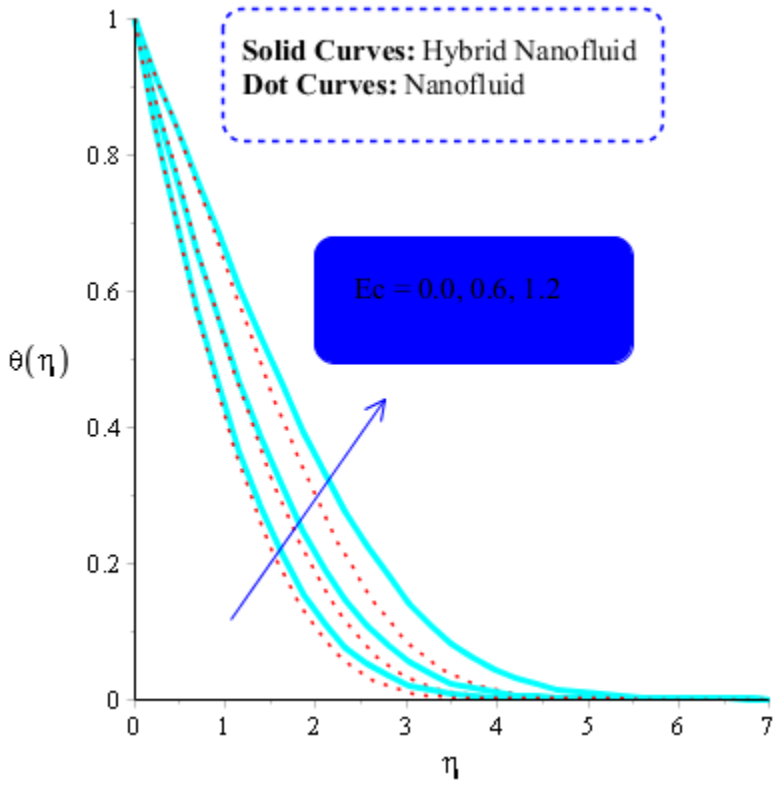

Figure 12: Influence of Ec on θ when $Du = 0.1, M = 0.2, Sc = 5,\ Pr = 4, (Gr)_c = 0.3, K^* = 0.1, \beta^* = 0.2, Sr = 0.1,\ (Gr)_t = 0.5, Du = 0.2, \epsilon_1 = 0.3, \epsilon_2 = 0.5, \alpha_1 = 0.5, \alpha_2 = 3.0.$

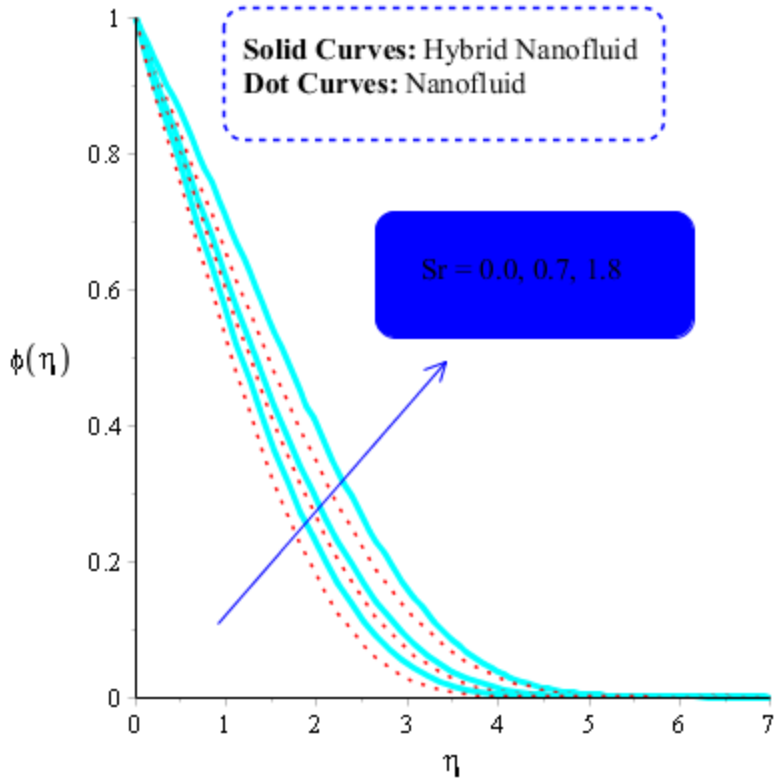

Figure 13: Influence of Sr on ϕ when $Du = 0.2, M = 0.5, Sc = 5, Pr = 4, (Gr)_c = 0.3, K^* = 0.1, \beta^* = 0.2, Ec = 0.001,$ and $(Gr)_t = 0.5, Du = 0.2, \epsilon_1 = 0.3, \epsilon_2 = 0.5, \alpha_1 = 0.5, \alpha_2 = 3.0$.

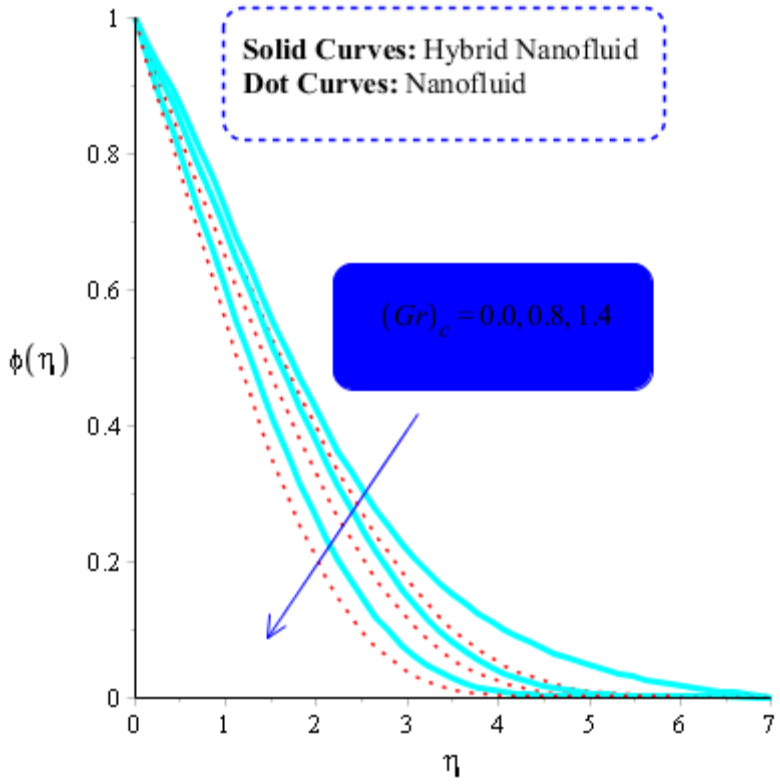

Figure 14: Influence of $(Gr)_c$on ϕ when $Du = 0.4, M = 0.6, Sr = 0.1,\ Pr = 5, Sc = 0.03,$ $K^* = 0.1, \beta^* = 0.2, Ec = 0.001,$ and $(Gr)_t = 0.5, Du = 0.2, \epsilon_1 = 0.3, \epsilon_2 = 0.5, \alpha_1 = 0.5, \alpha_2 = 3.0.$

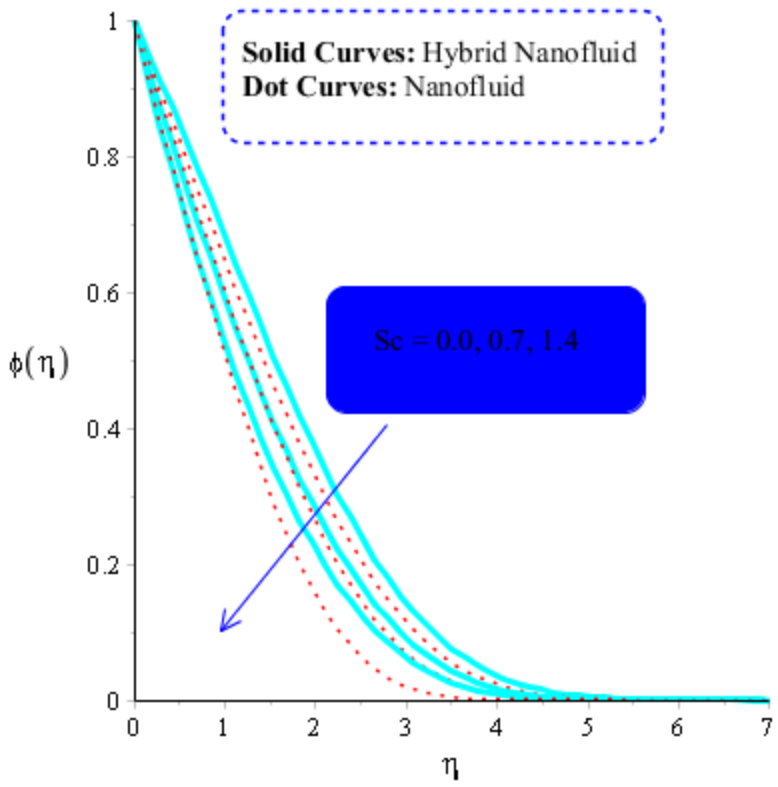

Figure 15: Influence of Sc on ϕ when $Du = 0.2, M = 0.7, Sr = 0.1, \beta = 0.2, Pr = 5, (Gr)_c = 0.3, K^* = 0.1, \beta^* = 0.2, Ec = 0.001,$ and $(Gr)_t = 0.5, Du = 0.5, \epsilon_1 = 0.3, \epsilon_2 = 0.5, \alpha_1 = 0.5, \alpha_2 = 3.0.$

Wall shear stresses, heat transfer rate and mass flux: Numerical data related to wall shear stresses in x and y-direction, wall heat transfer rate and wall mass flux for both types of fluids, Cu -fluid (mono nanofluid) and Cu - Ag -fluid (hybrid nanofluid) are investigated versus of variation of key parameters, k^*, Du, Sr and Sc (see Table 3). The numerical outcomes are summarized in Table 3. It appears that the k^* is inversely proportional to the voids present in porous medium. Hence, the resistive force per unit area (stress) increases. Therefore, wall shear stresses in both x and y-directions are increasing functions of k^*. Temperature gradient and mass-flux are both decreasing function of k^*. It is also observed that wall shear stress increases when Du is increased. On the other hand, a rise in wall mass flux against Du is noted. Finally, temperature gradient on solute particles is determined by Sr an increase Sr causes a decrease in wall shear stress, However, opposite trend is noted for Sc.

Table 3. Simulations of physical quantizes when $Du = 0.5, M = 0.8, Sr = 0.4, \beta = 0.2, Pr = 3, (Gr)_c = 0.5, K^* = 0.2, \beta^* = 1.2, Ec = 3, Sc = 7,$ and $(Gr)_t = 0.2$.

		$-C_{fx}(Re)^{1.5}$	$-C_{fy}(Re)^{1.5}$	$-Nu(Re)^{1.5}$	$-Sh(Re)^{1.5}$
	0.3	0.5854736654	0.4251622865	1.469615409	1.336014008
k^*	0.7	0.5908495342	0.5872447698	1.477060316	1.342782105
	0.9	0.6643955706	0.594703677	1.480258693	1.376598812
	0.2	0.5264339688	1.137228409	1.457396180	1.324905619
Du	0.5	0.5042650248	1.119093231	1.424234505	1.310213186
	1.3	0.5000114186	1.010257923	1.417014987	1.302740897
	0.0	0.5000114159	1.210257919	1.778926707	1.617206098
Sr	0.7	0.4856589213	1.138660768	1.726486241	1.604078401
	1.6	0.4835117384	1.108346245	1.718368259	1.525789326
	0.0	0.4835117388	1.238346247	2.235444588	2.032222353
Sc	0.7	0.4835117399	1.238346247	2.563934111	2.330849192
	1.5	0.4835117384	1.238346245	2.805765261	2.550695691

5. Core points and conclusions

The features of heat energy and mass diffusion inserting important role in the behavior of nanoparticles and hybrid nanostructures are addressed over the vertical 3D melting surface. Newtonian fluid under simultaneous influences of heat generation, porous medium, viscous dissipation, temperature gradient, rate of mass diffusion and Joule heating is considered. The prime findings are listed below:

1. Convergence study is tested observing by 300 elements;
2. Approach of Hybrid nanoparticles is estimated as efficient to achieve maximum production of energy into fluidic particles as compared for nanofluid;
3. Magnetic field parameter reduces motion of particles;

4. Maximum amount of thermal energy is achieved versus argument values of Eckert number, bouncy parameter and magnetic parameter ;
5. Role of variable thermal conductivity number rises growth of heat energy;
6. 300 elements are needed for mesh free analysis.

References

1. Dogonchi, AS.; Chamkha, AJ.; Seyyedi, SM.; Ganji, DD. Radiative nanofluid flow and heat transfer between parallel disks with penetrable and stretchable walls considering Cattaneo–Christov heat flux model. Heat Transfer—Asian Research. 2018 Jul;47(5):735-53.

2. Sadeghi, MS.; Tayebi, T.; Dogonchi, AS.; Armaghani, T.; Talebizadehsardari, P. Analysis of hydrothermal characteristics of magnetic Al2O3- H2O nanofluid within a novel wavy enclosure during natural convection process considering internal heat generation. Mathematical Methods in the Applied Sciences. 2020 May 25.

3. Nazir, U.; Sohail, M.; Alrabaiah, H.; Selim, MM.; Thounthong, P.; Park, C. Inclusion of hybrid nanoparticles in hyperbolic tangent material to explore thermal transportation via finite element approach engaging Cattaneo-Christov heat flux. Plos one. 2021 Aug 25;16(8):e0256302..

4. Ebrahimpour, Z.; Sheikholeslami, M.; Farshad, SA.; Shafee, A. Radiation heat transfer within a solar system considering nanofluid flow inside the absorber tube. International Journal of Numerical Methods for Heat & Fluid Flow. 2021 Mar 18.

5. Sheikholeslami, M.; Ganji. DD.; Ferrofluid convective heat transfer under the influence of external magnetic source. Alexandria engineering journal. 2018 Mar 1;57(1):49-60.
6. Ahmed, Z.; Bhargav, A.; Thermal interfacial resistance and nanolayer effect on the thermal conductivity of Al2O3-CO2 nanofluid: a molecular dynamics approach. arXiv preprint arXiv:2006.12805. 2020 Jun 23.

7. Saif, RS.; Hayat, T.; Ellahi, R.; Muhammad, T.; Alsaedi, A.; Darcy–Forchheimer flow of nanofluid due to a curved stretching surface. International Journal of Numerical Methods for Heat & Fluid Flow. 2018 Dec 14.

8. U. Nazir, N.H. Abu-Hamdeh, M. Nawaz, S.O. Alharbi. and W. Khan. "Numerical study of thermal and mass enhancement in the flow of Carreau-Yasuda fluid with hybrid nanoparticles". *Case Studies in Thermal Engineering (2021)*: 10125.

9. U. Nazir, M.A. Sadiq and M. Nawaz. "Non-Fourier thermal and mass transport in hybridnano-Williamson fluid under chemical reaction in Forchheimer porous medium". *International Communications in Heat and Mass Transfer (2021)*: 10553.

10. A. S. Dogonchi, K. Divsalar, and D. D. Ganji. "Flow and heat transfer of MHD nanofluid between parallel plates in the presence of thermal radiation." *Computer Methods in Applied Mechanics and Engineering* 310 (2016): 58-76.

11. A. J.Chamkha, A. S. Dogonchi, and D. D. Ganji. "Magneto-hydrodynamic flow and heat transfer of a hybrid nanofluid in a rotating system among two surfaces in the presence of thermal radiation and Joule heating." *AIP Advances* 9, no. 2 (2019): 025103.

12. S. Mosayebidorcheh, M. Sheikholeslami, M. Hatami, and D. D. Ganji. "Analysis of turbulent MHD Couette nanofluid flow and heat transfer using hybrid DTM–FDM." *Particuology* 26 (2016): 95-101.

13. M. Sheikholeslami, H. R. Kataria, and A. S. Mittal. "Effect of thermal diffusion and heat-generation on MHD nanofluid flow past an oscillating vertical plate through porous medium." *Journal of Molecular Liquids* 257 (2018): 12-25.

14. U. Nazir, M. Nawaz, M.M Alqarni and S. Saleem. "Finite element study of flow of partially ionised fluid containing nanoparticles". *Arabian Journal for Science and Engineering (2021)*: 10257-1026.

15. S. R. Sajjad, T. Muhammad, H. Sadia, and R. Ellahi. "Hydromagnetic flow of Jeffrey nanofluid due to a curved stretching surface." *Physica A: Statistical Mechanics and its Applications* 551 (2020): 124060.
16. U. Khan, A. Zaib, and F. Mebarek-Oudina, "Mixed convective magneto flow of SiO 2–MoS 2/C 2 H 6 O 2 hybrid nanoliquids through a vertical stretching/shrinking wedge: stability analysi." *Arabian Journal for Science and Engineering*, *45* (2020): 9061-9073.
17. Mebarek- Oudina, "Convective heat transfer of Titania nanofluids of different base fluids in a cylindrical annulus with a discrete heat source." *Heat Transfer—Asian Research*, *48*(1) (2019): 135-147.
18. K. Swain, F. Mebarek-Oudina, and M. S. Abo-Dahab. "Influence of MWCNT/Fe 3 O 4 hybrid nanoparticles on an exponentially porous shrinking sheet with chemical reaction and slip boundary conditions." *Journal of Thermal Analysis and Calorimetry*,(2021): 1-10.
19. A. Zaim, A. Aissa, F. Mebarek-Oudina, F, B. Mahanthesh, G. Lorenzini, M. Sahnoun, and M. El Ganaoui. "Galerkin finite element analysis of magneto-hydrodynamic natural convection of Cu-water nano liquid in a baffled U-shaped enclosure." *Propulsion and Power Research*, *9*(4) (2020): 383-393.
20. S. Marzougui, M. Bouabid, F. Mebarek-Oudina, N. Abu-Hamdeh, M. Magherbi, and K. Ramesh. "A computational analysis of heat transport irreversibility phenomenon in a magnetized porous channel." *International Journal of Numerical Methods for Heat & Fluid Flow* (2020).
21. R. Fares, F. Mebarek-Oudina, A. Aissa, M. S. Bilal, and F. H. Öztop. "Optimal entropy generation in Darcy-Forchheimer magnetized flow in a square enclosure filled with silver-based water nano liquid." *Journal of Thermal Analysis and Calorimetry*, 1-11: (2021).
22. M. S. Abo-Dahab, A.M. Abdelhafez, F. Mebarek-Oudina, and M. S. Bilal. "MHD Casson nanofluid flow over nonlinearly heated porous medium in presence of extending surface effect with suction/injection." *Indian Journal of Physics*, (2021): 1-15.
23. M.B. Hafeez, W. Sumelka, U. Nazir, H. Ahmad, and S. Aska. "Mechanism of Solute and Thermal Characteristics in a Casson Hybrid Nanofluid Based with Ethylene Glycol Influenced by Soret and Dufour Effects" . *Energies*, *14*(20) (2021): 6818.

24. M. Hafeez, R. Amin, K. Nisar, W. Jamshed, H. A. Abdel-Aty, and M. Khashan. "Heat transfer enhancement through nanofluids with applications in an automobile radiator." *Case Studies in Thermal Engineering, 27 (2021)*, 101192.

25. T. Hayat, and M. Nawaz. "Soret and Dufour effects on the mixed convection flow of a second grade fluid subject to Hall and ion- slip currents." *International Journal for Numerical Methods in Fluids* 67, no. 9 (2011): 1073-1099.

26. M. Nawaz, T. Hayat, and A. Alsaedi. "Dufour and Soret effects on MHD flow of viscous fluid between radially stretching sheets in porous medium." *Applied Mathematics and Mechanics* 33, no. 11 (2012): 1403-1418.

27. M. Subrata, S. Shaw, and G. C. Shit. "Fractional order model for thermochemical flow of blood with Dufour and Soret effects under magnetic and vibration environment." *Colloids and Surfaces B: Biointerfaces* 197 (2021): 111395.

28. W. Iskandar, A. Ishak, and I. Pop. "Dufour and Soret effects on Al2O3-water nanofluid flow over a moving thin needle: Tiwari and Das model." *International Journal of Numerical Methods for Heat & Fluid Flow* (2020).

29. K. Ambreen A. S. Naeem, R. Ellahi, Sadiq M. Sait, and K. Vafai. "Dufour and Soret effects on Darcy-Forchheimer flow of second-grade fluid with the variable magnetic field and thermal conductivity." *International Journal of Numerical Methods for Heat & Fluid Flow* (2020).

Author name Hasan Shahzad

Title of the article

Maximum Transportation Growth in Energy and Solute Particles in Prandtl Martial across a Vertical 3D-Heated Surface: Simulations Achieved using by Finite Element Approach

Signature Hasan Shahzad

Conflict of interest

The authors have no relevant of interest to disclose.